Carbohydrate Polymers 103 (2014) 62–69

Contents lists available at ScienceDirect

Carbohydrate Polymers

journal homepage: www.elsevier.com/locate/carbpol

Cellulose aerogel regenerated from ionic liquid solution for immobilized metal affinity adsorption

Tatsuya Oshima*, Toshihiko Sakamoto, Kaoru Ohe, Yoshinari Baba

Department of Applied Chemistry, University of Miyazaki, 1-1 Gakuen Kibanadai Nishi, Miyazaki 889-2192, Japan

ARTICLE INFO

Article history:
Received 28 September 2013
Received in revised form 4 December 2013
Accepted 7 December 2013
Available online 14 December 2013

Keywords:
Cellulose aerogel
Ionic liquids
Immobilized metal affinity
Adsorption
Protein

ABSTRACT

Surface morphology of cellulosic adsorbents is expected to influence the adsorption behavior of biomacromolecules. In the present study, cellulose aerogel regenerated from ionic liquid solution was prepared for use as a polymer support for protein adsorption. Iminodiacetic acid groups were introduced to the aerogel for immobilized metal affinity adsorption of proteins. A Cu(II)-immobilized iminodiacetic acid cellulose aerogel (Cu(II)-IDA-CA), which has a large specific surface area, showed a higher adsorption capacity than Cu(II)-immobilized iminodiacetic acid bacterial cellulose (Cu(II)-IDA-BC) and Cu(II)-immobilized iminodiacetic acid plant cellulose (Cu(II)-IDA-PC). In contrast, the Cu(II)-immobilized cellulosic adsorbents showed similar adsorption capacities for smaller amino acid and peptides. The results show that cellulose aerogels are useful as polymer supports with high protein adsorption capacities.

1. Introduction

The development of novel cellulosic materials has been revisited recently because of the discovery of new solvents for cellulose, such as ionic liquids (ILs) (El Seoud, Koschella, Fidale, Dorn, & Heinze, 2007; Feng & Chen, 2008), aqueous NaOH (Isogai & Atalla, 1998), and NaOH/urea (Cai & Zhang, 2005). Rogers and coworkers first reported dissolution of cellulose in IL (Ohno & Fukaya, 2009; Pinkert, Marsh, Pang, & Staiger, 2009; Swatloski, Spear, Holbrey, & Rogers, 2002; Wang, Gurau, & Rogers, 2012). In that study, 1-butyl-3-methylimidazolium chloride ([Bmim]Cl) showed the best cellulose solubility at 70–100 °C. Hydrogen bonding between chloride and the hydroxyl groups of cellulose is important for the dissolution. Furthermore, a new class of ILs for the dissolution of cellulose under mild conditions has been developed. Some ILs containing carboxylate ions can dissolve cellulose at room temperature through strong hydrogen-bonding basicity (Fukaya, Hayashi, Wada, & Ohno, 2008). Dissolution of cellulose in ILs has attracted significant attention from the viewpoint of energy generation from biomass resources (FitzPatrick, Champagne, Cunningham, & Whitney, 2010; Liu, Wang, Stiles, & Guo, 2012; Mäki-Arvela, Anugwom, Virtanen, Sjöholm, & Mikkola, 2010). In addition, novel materials have been developed through regeneration of cellulose from IL solutions (Lin, Zhan, Liu, Fu, & Lucia, 2009).

Regenerated cellulose films have been prepared from IL solutions by many researchers (Cao, Li, Zhang, Zhang, & He, 2010; Liu et al., 2011; Ma, Zhou, Li, Li, & Ou, 2011; Turner, Spear, Holbrey, & Rogers, 2004; Turner, Spear, Holbrey, Daly, & Rogers, 2005; Zhang et al., 2007). Rogers and co-workers developed IL-regenerated cellulose membranes as a solid support for enzymes (Turner et al., 2004; Turner et al., 2005). Catalytic activities of laccase immobilized on regenerated cellulose films were studied. Composite films composed of nanocrystalline cellulose and a cellulose matrix regenerated from IL (1-(2-hydroxylethyl)-3-methyl imidazolium chloride) solution were also developed (Ma et al., 2011). These nanocomposite films showed optical transparency, thermal stabilities and mechanical properties as the result of reinforcement by increasing the content of nanocrystalline cellulose. Electrospinning of cellulose from IL solutions to prepare cellulose nanofibers has also been examined (Härdelin et al., 2012; Meli, Miao, Dordick, & Linhardt, 2010; Quan, Kang, & Chin, 2010; Viswanathan et al., 2006; Xu et al., 2008). The typical diameter of electrospun cellulose fibers is in the range 120–800 nm (Meli et al., 2010; Quan et al., 2010). A gel material composed of cellulose, the ionic liquid, and water was also developed from an IL solution of cellulose (Kadokawa, Murakami, & Kaneko, 2008).

Cellulose aerogels (CAs) can be obtained by dissolution of cellulose, followed by regeneration. CAs are highly porous materials with pore sizes partly in the nanometer-region (Jin, Nishiyama, Wada, & Kuga, 2004; Innerlohinger, Weber, & Kraft, 2006). Highly porous aerogels consisting of cellulose nanofibrils were prepared by dissolution/regeneration of cellulose in aqueous calcium thiocyanate, followed by regeneration and controlled drying (Jin

* Corresponding author. Tel.: +81 985 58 7321; fax: +81 985 58 7323.
E-mail address: oshimat@cc.miyazaki-u.ac.jp (T. Oshima).

0144-8617/$ – see front matter © 2013 Elsevier Ltd. All rights reserved.
http://dx.doi.org/10.1016/j.carbpol.2013.12.021

et al., 2004). The resulting aerogels had highly porous networks composed of nanometer-sized cellulose fibrils. CAs have also been prepared from cellulose-*N*-methyl-morpholine-*N*-oxide (NMMO) solutions and cellulose-lithium chloride/dimethyl sulfoxide (LiCl/DMSO) solutions (Wang, Liu, Matsumoto, & Kuga, 2012). Aaltonen and co-workers recently reported the preparation of lignocellulosic aerogels from ionic liquid solutions (Aaltonen & Jauhiainen, 2009; Deng, Zhou, Du, van Kasteren, & Wang, 2009). Their CAs consisted of a nanofibrillar biomaterial network with an open-pore structure. Recently, CAs functionalized with silver nanoparticles have been developed (Dong, Snyder, Tran, & Leadore, 2013). CAs are novel materials, expected to have a variety of uses because of their highly porous structures and large surface areas.

In the present study, CA was prepared by regeneration of cellulose from an IL solution for use as a polymer support for immobilized metal affinity chromatography (IMAC) of proteins. IMAC is a biomolecule separation technique based on the metal chelate interaction between coordinating groups in the biomolecules and metal ions immobilized on an adsorbent (Chaga, 2001; Porath, 1992; Porath, Carlsson, Olsson, & Belfrage, 1975). The protein separation factor of IMAC is dominated by the affinities between immobilized metal ions and functional groups on the biomolecules. Transition metal ions such as Cu(II), Ni(II), Co(II), and Zn(II) immobilized to metal-chelating groups on the adsorbent interact with amino acid side chains such as histidine residues. IMAC is currently applied for the purification of recombinant proteins. Recombinant proteins fused with peptide tags containing multiple histidine residues (metal affinity sites) on their C- or N-terminus are selectively recovered by immobilized metal chelating gels, often in a single chromatographic step. The polymeric support for IMAC must satisfy many requirements, including (i) easy derivatization, (ii) low non-specific adsorption, (iii) good physical, mechanical and chemical stability, and (iv) high porosity for easy ligand accessibility (Ueda, Gout, & Morganti, 2003). Hence, cellulose and crosslinked agarose have been used as polymer supports for IMAC. Additionally, the surface morphology of cellulosic adsorbents influences the protein adsorption capacity (Anirudhan, Rejeena, & Binusree, 2013). The authors reported adsorption of proteins on phosphorylated bacterial cellulose (Oshima, Kondo, Ohto, Inoue, & Baba, 2008; Oshima, Taguchi, Ohe, & Baba, 2011). Bacterial cellulose (BC, also known as microbial cellulose) is extracellular cellulose synthesized by bacteria such as *Acetobacter xylinum*, and the fine network structure of BC holds a large quantity of biomacromolecules, because of its large surface area (Chen et al., 2013; Iguchi, Yamanaka, & Budhiono, 2000; Kalashnikova, Bizot, Cathala, & Capron, 2011). The adsorption capacity of phosphorylated bacterial cellulose is much higher than that of phosphorylated plant cellulose, despite their similar phosphorylation degree. Similarly, the adsorption capacity for hemoglobin on quaternary ammonium BC is higher than on quaternary ammonium plant cellulose prepared under the same conditions (Niide et al., 2010). Recently, iminodiacetic acid BC (IDA-BC) was prepared for IMAC of proteins (Sakamoto, Oshima, Taguchi, Ohe, & Baba, 2010). The adsorption capacities of Cu(II)-immobilized IDA-BC (Cu(II)-IDA-BC) for proteins was higher than that of Cu(II)-immobilized iminodiacetic acid plant cellulose (Cu(II)-IDA-PC).

In this paper, iminodiacetic acid CA (IDA-CA), IDA-BC, and IDA-PC were prepared in a similar manner using different cellulosic materials. Adsorption capacities of Cu(II)-immobilized IDA-CA (Cu(II)-IDA-CA), Cu(II)-IDA-BC, and Cu(II)-IDA-PC for various biomolecules were compared to study the effect of the cellulosic support structure. Adsorbed biomolecules hemoglobin, myoglobin, lysozyme, angiotensin I, carnosine, and histidine differ in size (molecular weight). The relationship between the surface morphology of the cellulosic adsorbents and the size of adsorbed biomolecules was studied using adsorption isotherms.

2. Experimental

2.1. Materials

Microcrystalline plant cellulose powder C (PC) was purchased from AdvantecToyo Kaisha, Ltd., Tokyo, Japan. This powder is made from high purity cotton cellulose, treated with an acid to remove ash. PC was used as a starting material to prepare CA and IDA-PC. The BC starting material was prepared from "nata de coco" by grinding, washing with distilled water, and lyophilization. According to a previous paper, number and weight average molecular mass (Mn and Mw, respectively) of PC are 3.75×10^4 and 5.86×10^4 (Yanagisawa, Shibata, & Isogai, 2004). 1-Butyl-3-methylimidazolium chloride ([Bmim]Cl), used as the IL in this study, was synthesized according to the procedures described in a previous paper (Dupont et al., 2002). The following reagents for adsorption experiments were used as received: hemoglobin from bovine blood, myoglobin from equine skeletal muscle, angiotensin I (Asp-Arg-Val-Tyr-Ile-His-Pro-Phe-His-Leu), L-histidine (His, Wako Pure Chemical Industries, Osaka, Japan), L-carnosine (β-alanyl-L-histidine, Car, Sigma–Aldrich Co., St Louis, MO, USA), and lysozyme from chicken egg white (Nacalai Tesque Inc., Kyoto, Japan). All other reagents were reagent grade and were used as received.

2.2. Preparation of cellulose aerogel (CA)

CA was prepared in a similar manner to that described previously, as follows (Deng et al., 2009; Jin et al., 2004): PC, which is made from high purity cotton cellulose, was used as the starting material of CA. Dry PC (4.0 g) and [Bmim]Cl (45.7 g) were mixed in a flask. The mixture was stirred at 100 °C for 24 h to obtain a transparent solution. The mixture was cast onto a glass dish and cooled to room temperature. The mixture was coagulated by immersing in methanol, followed by tert-butanol. The resulting gel was washed using distilled water until no chloride ions were detected using $AgNO_3$. The resulting gel was ground and used as CA. After rapid freezing using liquid nitrogen, the ground wet gel was lyophilized to obtain dry CA. The crystal structures of PC and CA were examined using XRD (RINT2000, Rigaku, Tokyo, Japan).

2.3. Preparation of IDA-CA, IDA-BC, and IDA-PC

IDA-CA was prepared according to the scheme shown in Fig. 1 as follows (Kanemaru, Oshima, & Baba, 2010; Sakamoto et al., 2010): 4.0 g of CA was swelled using 600 cm^3 of distilled water containing 33% (v/v) ethanol. After the mixture was stirred for 24 h, 40 cm^3 of epichlorohydrin (360 mmol) was added to the mixture. After about 30 min, 40 cm^3 of 5.0 M NaOH aqueous solution was added to the mixture. The mixture was stirred at 60 °C for 1 h. After cooling, the mixture was filtered and the residue was washed with distilled water. To the residue, 750 cm^3 of distilled water containing 97.5 g (550 mmol) disodium iminodiacetate monohydrate and 50 g sodium carbonate was added in a reaction flask. The mixture was stirred at 80 °C for 24 h. After cooling, the mixture was filtered and washed using distilled water until the filtrate became neutral. The residue was immersed in methanol and subsequently in tert-butanol for 24 h. After filtration, the residue was lyophilized to obtain IDA-CA as a powdery white material. Iminodiacetic acid bacterial cellulose (IDA-BC) and iminodiacetic acid plant cellulose (IDA-PC) as references for IDA-CA were prepared in a similar manner to that of IDA-CA, from BC and PC respectively. IDA-CA, IDA-BC, and IDA-PC were observed with scanning electron microscope (KEYENCE VE-8800, Osaka, Japan, and HITACHI S-5500, Tokyo, Japan) to evaluate the morphology. The specific surface areas of IDA-CA, IDA-BC, and IDA-PC were determined by the N_2-BET

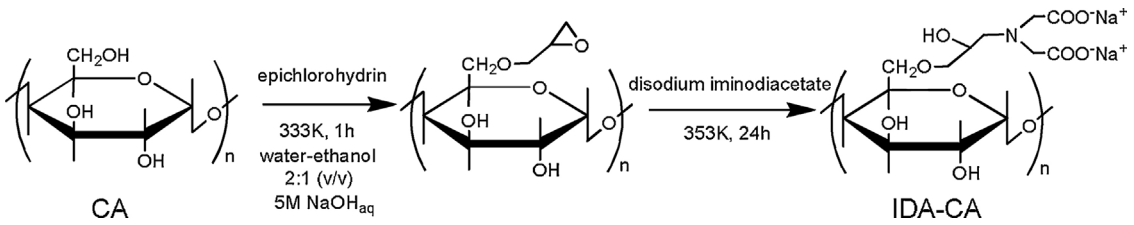

Fig. 1. The preparation scheme for IDA-CA (IDA-BC and IDA-PC).

method using a volumetric adsorption measurement instrument (BEL Japan BELSORP max, Osaka, Japan).

2.4. Preparation of Cu(II) immobilized IDA-CA (Cu(II)-IDA-CA)

Cu(II) immobilized IDA-CA (Cu(II)-IDA-CA) was prepared by adsorption of Cu(II) on IDA-CA as follows (Kanemaru et al., 2010; Sakamoto et al., 2010). An aqueous solution containing 5.0 mM $Cu(NO_3)_2$ was prepared and the pH adjusted to 5.0 using 100 mM HEPES buffer and aqueous NaOH solution. A 200 cm^3 portion of the aqueous solution and 1.0 g of IDA-CA were mixed in a beaker, then stirred (150 rpm) at room temperature. A small amount of 100 mM aqueous NaOH solution was occasionally added to the mixture to keep the pH at about 5. After 20 h, the adsorption reached equilibrium and the mixture was filtered to collect the adsorbent. The residue was immersed in methanol and subsequently in tert-butanol for 24 h. After filtration, the residue was lyophilized to obtain Cu(II)-IDA-CA. Cu(II) immobilized IDA-BC (Cu(II)-IDA-BC) and Cu(II) immobilized IDA-PC (Cu(II)-IDA-PC) as references were prepared in a similar manner to that of Cu(II)-IDA-CA, from IDA-BC and IDA-PC respectively. Additionally, Cu(II)-IDA-CA, Cu(II)-IDA-BC, and Cu(II)-IDA-PC with different quantities of immobilized Cu(II) were also prepared by changing the initial concentration of Cu(II) in the solution.

The quantity of Cu(II) immobilized on the adsorbents was determined as follows. 10 mg of the adsorbents (Cu(II)-IDA-CA, Cu(II)-IDA-BC, or Cu(II)-IDA-PC) and 15 cm^3 of 1.0 M hydrochloric acid were mixed in a stoppered glass sample tube and shaken in a thermostatically controlled shaker (120 rpm) at 30 °C. After 20 h, Cu(II) ions were completely eluted from the adsorbents. After filtration of the mixture, the concentration of Cu(II) in the filtrate was analyzed using an atomic absorption spectrophotometer (PerkinElmer AAnalyst 100, CT, USA).

2.5. Adsorption of proteins, peptides, and an amino acid onto Cu(II) immobilized cellulose adsorbents

Experiments on the adsorption of proteins, peptides, and an amino acid onto Cu(II) immobilized cellulose adsorbents were carried out using a batchwise method as follows (Oshima et al., 2011). Aqueous solutions containing varying concentrations of hemoglobin (0.3–20 μM), myoglobin (1.0–150 μM), lysozyme (2.3–190 μM), angiotensin I (94–749 μM), Car (7.6–1070 μM), His (0.4–725 μM), in 100 mM sodium phosphate buffer solution (pH 8.0) were prepared. A portion (5.0 cm^3 for angiotensin I, 15 cm^3 for others) of each aqueous solution and 20 mg of an adsorbent (Cu(II)-IDA-CA, Cu(II)-IDA-BC, or Cu(II)-IDA-PC) were mixed in a stoppered glass tube and shaken at 120 rpm in a thermostat-regulated shaker at 30 °C. After 24 h, adsorption equilibrium was attained and the mixture was filtered. The concentrations of residual hemoglobin, myoglobin, lysozyme, and angiotensin I in the filtrate were determined with a UV-VIS spectrophotometer (JASCO V-660, Tokyo, Japan). The concentrations of residual Car and His were determined with a Shimadzu Prominence HPLC Amino Acid Analysis System (Shimadzu, Kyoto, Japan). The analysis system was based on a gradient reversed-phase HPLC using a Shimadzu LC-20AB as a pump (flow rate: 0.6 cm^3 min^{-1}) and equipped with a Shimadzu Shim-pack Amino Li as a column. Post-column fluorescence detection of the o-phtalaldehyde (OPA) amino acid derivative was done with a Shimadzu RF-10AXL fluorescence detector (Ex: 350 nm, Em: 450 nm). Moreover, concentrations of Cu(II) ions that had eluted from the Cu(II) immobilized adsorbents were analyzed using an atomic absorption spectrophotometer (PerkinElmer AAnalyst 100). From the concentrations of adsorbates before and after adsorption, the percentage adsorption (Adsorption [%]) and the quantity adsorbed (q [μmol g^{-1}]) were calculated according to the following equations;

$$\text{Adsorption} = \frac{C_0 - C_e}{C_0} \times 100\,[\%]$$

$$q = \frac{C_0 - C_e}{W} \times V\,[\mu\text{mol}\,g^{-1}]$$

where C_0 and C_e are the concentrations of adsorbates before and after adsorption in μM, W is the dry mass of adsorbent in g, and V is the volume of solution in dm^3.

3. Results and discussion

3.1. Characterization of iminodiacetic acid cellulosic adsorbents

In the present study, CA was prepared similarly to a previously reported method, by regeneration of cellulose from a [Bmim]Cl solution (Deng et al., 2009; Jin et al., 2004). From the results of preliminary experiments, 8 wt% cellulose solution in [Bmim]Cl was satisfactory for preparing a highly porous material. The solvent used for regeneration is also important for obtaining a porous material. In this case, methanol and tert-butanol were used and the resulting material was washed with distilled water (Jin et al., 2004). The resulting CA was soft and compressible, while the crystalline structure evaluated using X-ray diffractometer was destroyed compared with that of the starting material, PC (Aaltonen & Jauhiainen, 2009). After introduction of iminodiacetic acid groups, the sponge-like structure of the resulting IDA-CA was retained. Scanning electron micrographs of IDA-CA, IDA-BC, and IDA-PC at 10,000× magnification, as well as IDA-CA at 40,000× magnification, are shown in Fig. 2. The surface morphologies of the cellulosic materials differed markedly. A sponge-like porous structure can be observed on the surface of IDA-CA, with a pore size of less than 100 nm, whereas a microfibrous ribbon structure can be observed on the surface of IDA-BC, originating from the starting material, BC. In contrast, the surface structure of IDA-PC is flat, similar to the starting material, PC. Thus, the procedure of chemical modification seems to have little effect on surface morphology, nonetheless epichlorohydrine would also act as crosslinker (Iguchi et al., 2000; Oshima et al., 2011). The specific surface areas of iminodiacetic acid cellulose, determined using the N_2-BET method, were 355 m^2 g^{-1} for IDA-CA, 24 m^2 g^{-1} for IDA-BC, and 1.4 m^2 g^{-1} for IDA-PC. IDA-CA showed the largest specific surface area amongst the iminodiacetic acid

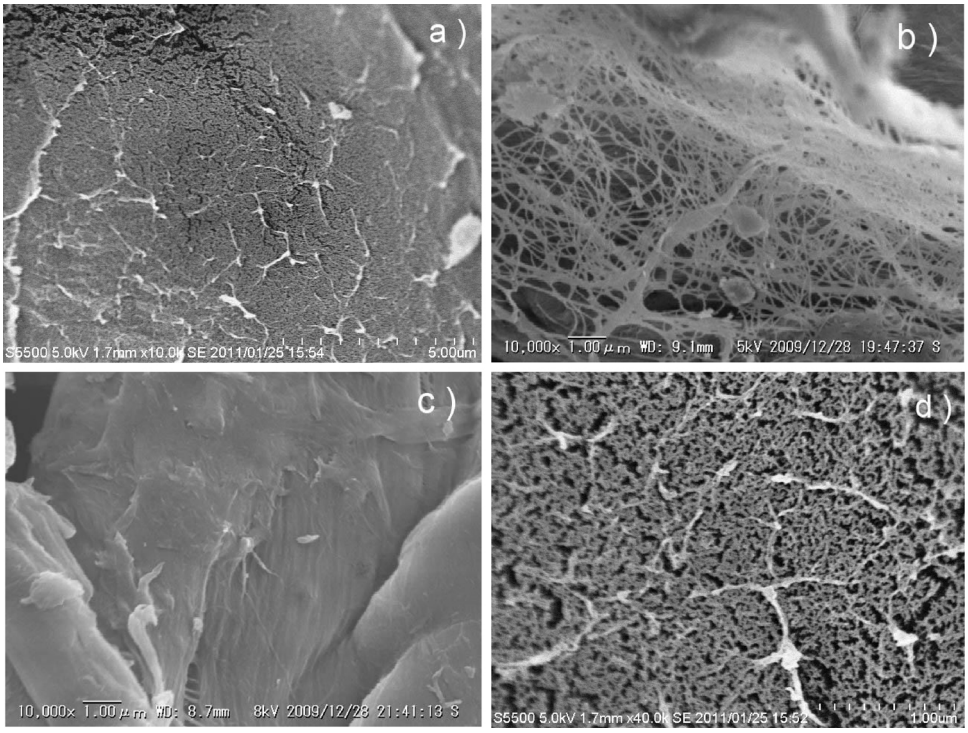

Fig. 2. Scanning electron micrographs of IDA-CA (a), IDA-BC (b), IDA-PC (c) at 10,000× magnification, and IDA-CA (d) at 40,000× magnification.

cellulose adsorbents prepared, ahead of IDA-BC. The change of IR (infrared) spectrum for IDA-CA compared with that for CA was small because of the small substitution degree. The substitution degree of iminodiacetic acid group onto IDA-CA was estimated from the maximum adsorption capacity of Cu(II), which is not adsorbed on CA: As the maximum adsorption capacity of Cu(II) on IDA-CA was 123 μmol g^{-1}, a similar quantity of iminodiacetic acid group should be introduced onto IDA-CA. Cu(II) immobilized iminodiacetic acid cellulose with different quantities of immobilized Cu(II) were prepared by changing the initial concentration of Cu(II). Immobilization of Cu(II) onto cellulosic adsorbents seems to be less influential to the morphology: The specific surface area of Cu(II)-IDA-CA was 328 m^2 g^{-1}, which is slightly smaller that of IDA-CA (355 m^2 g^{-1}).

3.2. Adsorption of proteins, peptides, and an amino acid onto Cu(II) immobilized cellulose adsorbents

In immobilized metal affinity adsorption, protein is adsorbed on adsorbents by the coordination bonding between metal ions immobilized on the adsorbents and amino acid side chains such as histidine residues (Chaga, 2001; Porath, 1992; Porath et al., 1975). Adsorption of hemoglobin onto Cu(II)-IDA-CA, on which different quantities of Cu(II) were immobilized, was examined to study the relationship between the adsorption capacity and the quantity of immobilized Cu(II). Fig. 3 shows the adsorption isotherms of hemoglobin on Cu(II)-IDA-CA at pH 7.9. The adsorbents differed with respect to the quantity of Cu(II) immobilized, specifically 17, 37, 66, 97, and 123 μmol g^{-1}. The quantity of hemoglobin adsorbed on Cu(II)-IDA-CA increased with an increase in the equilibrium concentration of hemoglobin but was asymptotic at different values. In addition, adsorption increased with increasing immobilized Cu(II) on Cu(II)-IDA-CA. The equilibrium experimental data was correlated with the Langmuir isotherm model, used to determine the maximum adsorption capacities of hemoglobin on Cu(II)-IDA-CAs (q_{max}) (Oshima et al., 2011). The Langmuir model assumes monolayer adsorption, as expressed by the following formula:

$$\frac{Ce}{q} = \frac{Ce}{q_{max}} + \frac{1}{q_{max}K}$$

where q denotes the quantity of hemoglobin adsorbed on Cu(II)-IDA-CA [μmol g^{-1}], C_e is the equilibrium concentration of hemoglobin in the aqueous solution [μmol dm^{-3}], and K_L is the adsorption equilibrium constant [dm^3 μmol^{-1}]. The theoretical adsorption isotherms calculated from the Langmuir isotherm model are shown in Fig. 3. Because the calculated values agreed with the experimental data, the adsorption of hemoglobin proceeds according to monolayer adsorption via coordination bonding between Cu(II) and amino acid residues such as histidine (Chaga, 2001; Porath, 1992). The q_{max} values of lysozyme on Cu(II)-IDA-CAs immobilized with above quantities of Cu(II) were evaluated as 0.89, 2.78, 5.69, 8.49, and 10.9 μmol g^{-1}, respectively.

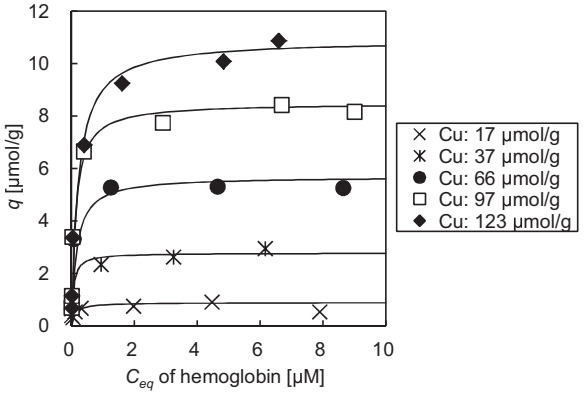

Fig. 3. Adsorption isotherms for hemoglobin onto Cu(II)-IDA-CAs immobilized with differing quantities of Cu(II) at 30 °C: pH_{eq} 7.92 ± 0.04; adsorbent, 10 mg; volume, 15 cm^3.

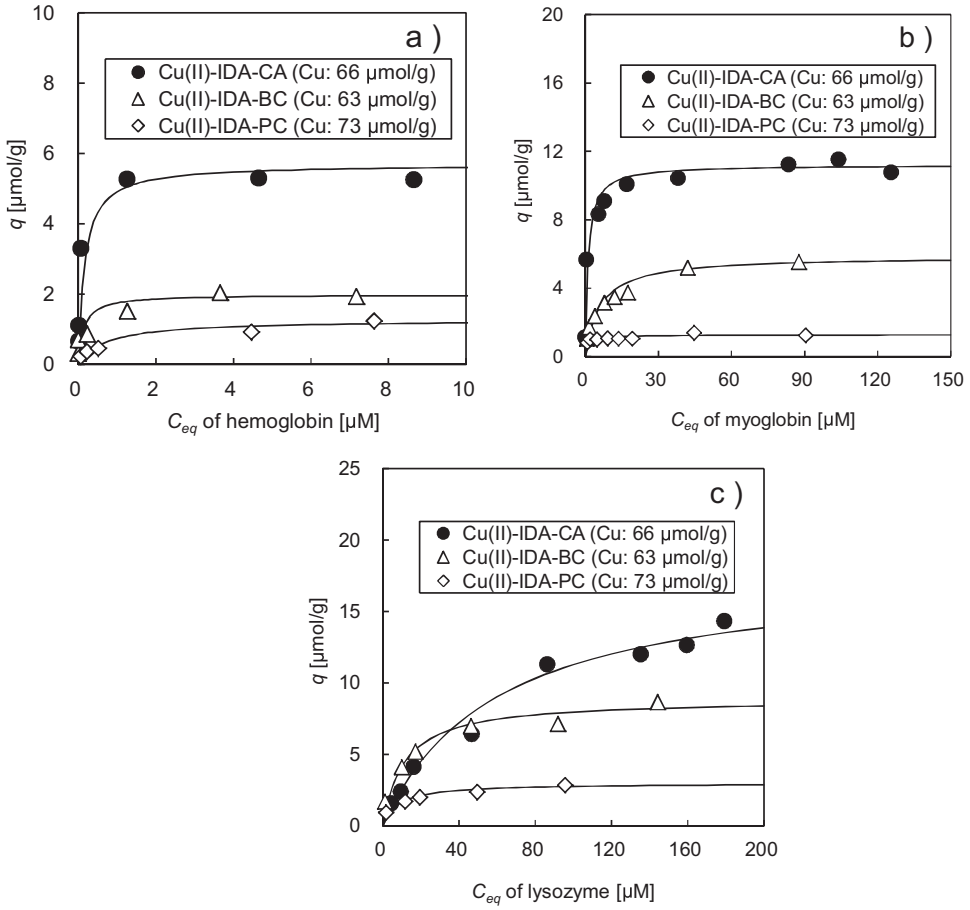

Fig. 4. Adsorption isotherms for proteins onto Cu(II)-IDA-CA, Cu(II)-IDA-BC, and Cu(II)-IDA-PC at 30 °C; (a) hemoglobin; (b) myoglobin; (c) lysozyme: pH_{eq} 7.97 ± 0.07; adsorbent, 10 mg; volume, 15 cm^3.

The adsorption behavior of proteins, peptides, and an amino acid, with a variety of molecular weights, were investigated. Specifically, immobilized metal affinity adsorption of hemoglobin (M.W. 64500 g/mol), myoglobin (17000 g/mol), lysozyme (14300 g/mol), angiotensin I (1296 g/mol), Car (226 g/mol), and His (155 g/mol), using Cu(II)-immobilized cellulose adsorbents Cu(II)-IDA-CA, Cu(II)-IDA-BC, and Cu(II)-IDA-PC was examined. Generally, His residues are the most important for IMAC adsorption because of their high affinity for transition metal ions (Chaga, 2001; Porath, 1992). Hemoglobin and myoglobin have multiple His residues (36 and 11, respectively). Lysozyme, angiotensin I, and Car have a single His residue. Cu(II) exhibits a relatively strong affinity for histidine residues and captures various proteins that contain a small number of histidine residues. Hence, the adsorbates in this study could be adsorbed on the Cu(II) immobilized cellulose adsorbents (Kanemaru et al., 2010; Sakamoto et al., 2010). The adsorption experiments were demonstrated at pH 8.0, at which metal affinity adsorption is generally conducted.

Fig. 4 shows adsorption isotherms of hemoglobin, myoglobin, and lysozyme onto Cu(II)-IDA-CA, Cu(II)-IDA-BC, and Cu(II)-IDA-PC. The adsorbents differed with respect to surface morphology but were rather similar in the quantity of Cu(II) immobilized; 66 μmol g^{-1} for Cu(II)-IDA-CA, 63 μmol g^{-1} for Cu(II)-IDA-BC, and 73 μmol g^{-1} for Cu(II)-IDA-PC. The quantity of proteins adsorbed on the Cu(II) immobilized cellulose adsorbents increased with increasing equilibrium concentration. It should be noted that the quantities of proteins adsorbed onto the adsorbents differed, despite the similar quantities of immobilized Cu(II). Cu(II)-IDA-CA showed the highest adsorption capacity for all proteins amongst the Cu(II) immobilized cellulose adsorbents tested in this study, followed by Cu(II)-IDA-BC. In contrast, the adsorption capacities using Cu(II)-IDA-PC were much lower than those of Cu(II)-IDA-CA and Cu(II)-IDA-BC. The equilibrium experimental data were correlated with the Langmuir isotherm model and the theoretical adsorption isotherms calculated from the Langmuir isotherm model are shown in Fig. 4. The calculated values agreed with experimental data.

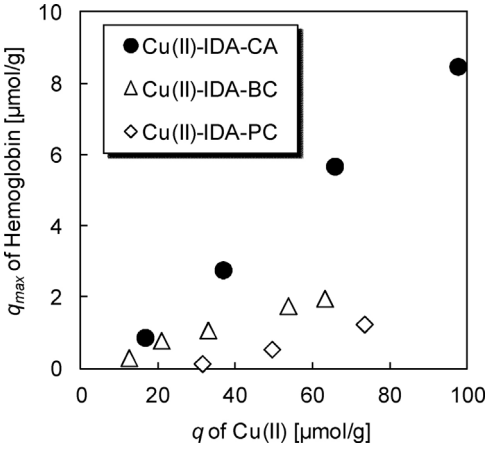

Fig. 5. Relationship between the amount of Cu(II) immobilized on Cu(II)-IDA-CA, Cu(II)-IDA-BC, and Cu(II)-IDA-PC and the maximum adsorption capacity for hemoglobin.

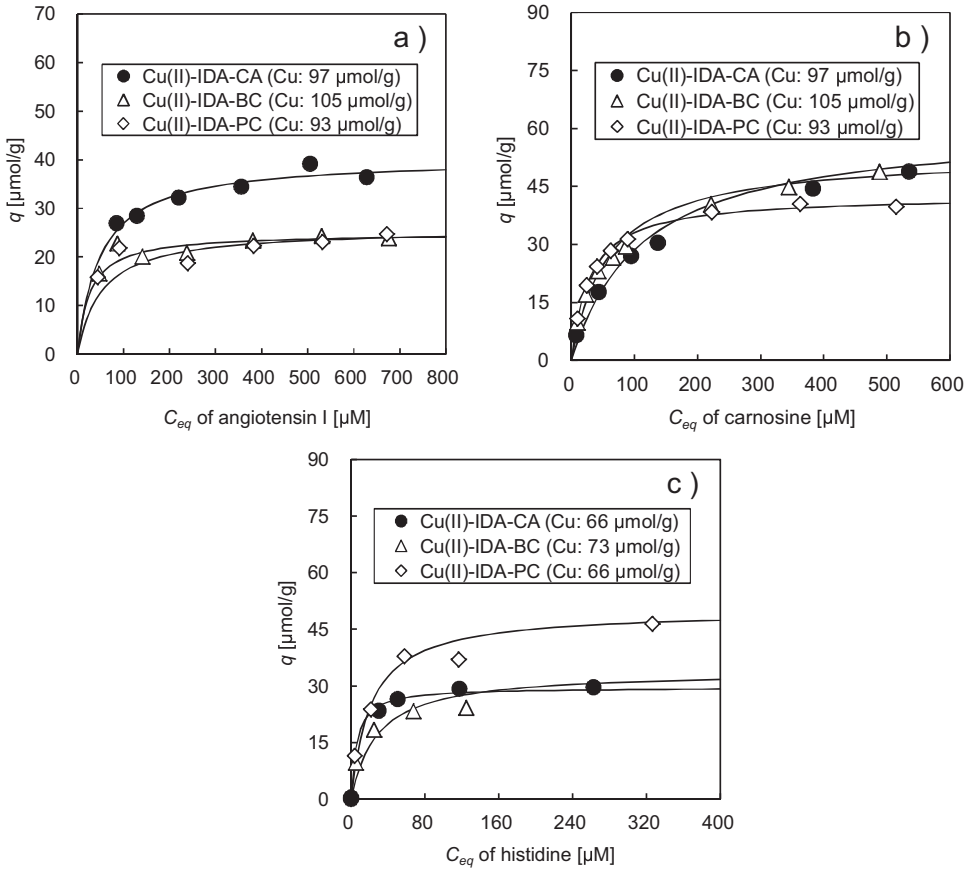

Fig. 6. Adsorption isotherms of peptides and an amino acid onto Cu(II)-IDA-CA, Cu(II)-IDA-BC, and Cu(II)-IDA-PC at 30 °C; (a) angiotensin I; (b) carnosine; (c) histidine: pH_{eq} 7.67 ± 0.20; adsorbent, 10 mg; volume, 5.0 cm^3 (a) or 15 cm^3 (b and c).

The relationship between the amounts of Cu(II) immobilized on Cu(II)-IDA-CA, Cu(II)-IDA-BC, and Cu(II)-IDA-PC and the maximum adsorption capacities for hemoglobin is shown in Fig. 5. The q_{max} values of hemoglobin increased with increasing quantities of immobilized Cu(II). The q_{max} values of Cu(II)-IDA-CAs were the highest amongst the adsorbents, followed by Cu(II)-IDA-BCs. The q_{max} values of Cu(II)-IDA-PCs were the lowest amongst the Cu(II) immobilized adsorbents. The order of q_{max} values for hemoglobin is consistent with order of specific surface areas of the adsorbents, suggesting that the surface morphology of the cellulosic adsorbents influences protein adsorption capacity.

Fig. 6 shows adsorption isotherms for angiotensin I, Car, and His onto Cu(II)-IDA-CA, Cu(II)-IDA-BC, and Cu(II)-IDA-PC, as well as the theoretical adsorption isotherms calculated from the Langmuir isotherm model. The quantity of Cu(II) immobilized on the adsorbents for the same adsorbates were closely similar; 97 μmol g^{-1} for Cu(II)-IDA-CA, 105 μmol g^{-1} for Cu(II)-IDA-BC, and 93 μmol g^{-1} for Cu(II)-IDA-PC (for adsorption of angiotensin I and Car); and 66 μmol g^{-1} for Cu(II)-IDA-CA, 63 μmol g^{-1} for Cu(II)-IDA-BC, and 73 μmol g^{-1} for Cu(II)-IDA-PC (for adsorption of His). Cu(II)-IDA-CA showed the highest adsorption capacity for angiotensin I, while the adsorption capacities for angiotensin I using Cu(II)-IDA-BC and Cu(II)-IDA-PC were similar. The adsorption capacities for Car using Cu(II)-IDA-CA, Cu(II)-IDA-BC, and Cu(II)-IDA-PC were similar. For adsorption of His, Cu(II)-IDA-PC showed higher adsorption capacity compared with Cu(II)-IDA-CA and Cu(II)-IDA-BC. The results for adsorption of peptides and His in contrast to those for adsorption of proteins, in which the order of adsorption capacities was clearly Cu(II)-IDA-CA > Cu(II)-IDA-BC > Cu(II)-IDA-PC.

The relationship between the amount of Cu(II) immobilized on Cu(II)-IDA-CA, Cu(II)-IDA-BC, and Cu(II)-IDA-PC and the maximum adsorption capacities for Car is shown in Fig. 7. The q_{max} values for Car increased with increasing quantities of immobilized Cu(II). In contrast to the adsorption of hemoglobin (Fig. 5), the q_{max} values for Car were similar on the three adsorbents. These results suggest that the surface morphology of the cellulosic adsorbents has less influence on the adsorption capacity of smaller amino acids.

Molecular information (molecular weight and number of His residues) for the biomolecules, their initial concentrations,

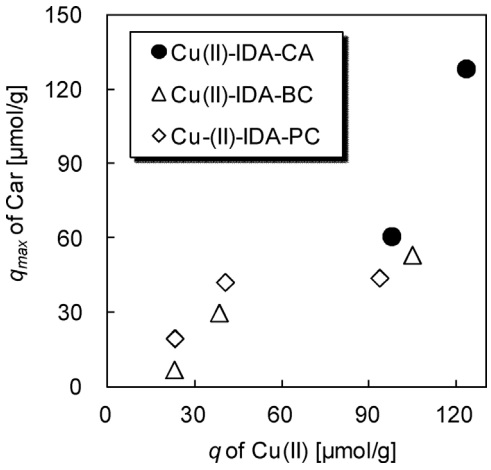

Fig. 7. Relationship between the amount of Cu(II) immobilized on Cu(II)-IDA-CA, Cu(II)-IDA-BC, and Cu(II)-IDA-PC and the maximum adsorption capacity for Car.

Table 1
The maximum adsorption capacities of proteins, peptides, and an amino acid onto Cu(II)-IDA-CA, Cu(II)-IDA-BC, and Cu(II)-IDA-PC.

Adsorbent	Material	Hemoglobin	Myoglobin	Lysozyme	Angiotensin I	Car	His
	M.W. [g mol^{-1}]	64,500	17,200	14,300	1296	226	155
	Number of His residues	36	11	1	1	1	1
	Initial conc.	0.3–10 [μmol dm^{-3}]	1.0–100 [μmol dm^{-3}]	3.0–150 [μmol dm^{-3}]	100–760 [μmol dm^{-3}]	10–500 [μmol dm^{-3}]	10–700 [μmol dm^{-3}]
Cu(II)-IDA-CA (355 [m^2 g^{-1}])[a]	q_{max} [μmol g^{-1}]	5.69	11.2	18.0	40.3	60.8	29.6
	(q of Cu(II) [μmol g^{-1}])[b]	(66)	(66)	(66)	(97)	(97)	(66)
Cu(II)-IDA-BC (24 [m^2 g^{-1}])[a]		1.98	5.86	8.87	24.9	53.3	33.9
		(63)	(63)	(63)	(105)	(105)	(63)
Cu(II)-IDA-PC (1.4 [m^2 g^{-1}])[a]		1.26	1.27	2.99	25.8	42.6	49.9
		(73)	(73)	(73)	(93)	(93)	(73)
$q_{max\ (Cu(II)\text{-}IDA\text{-}CA)}/q_{max\ (Cu(II)\text{-}IDA\text{-}BC)}$		2.86	1.91	2.03	1.62	1.14	0.87
$q_{max\ (Cu(II)\text{-}IDA\text{-}CA)}/q_{max\ (Cu(II)\text{-}IDA\text{-}PC)}$		4.52	8.82	6.02	1.56	1.42	0.59

[a] The values in parentheses show the specific surface areas of iminodiacetic acid celluloses.
[b] The values in parentheses show the amount of Cu(II) immobilized on the adsorbents.

and the maximum adsorption capacities for the biomolecules on Cu(II)-IDA-CA, Cu(II)-IDA-BC, and Cu(II)-IDA-PC, calculated using the Langmuir model from the experimentally determined adsorption isotherms using each adsorbent, are summarized in Table 1. The q_{max} ratios for Cu(II)-IDA-CA to q_{max} for Cu(II)-IDA-BC (q_{max}(Cu(II)-IDA-CA)/q_{max}(Cu(II)-IDA-BC)) as well as the q_{max} ratios for Cu(II)-IDA-CA to q_{max} for Cu(II)-IDA-PC (q_{max}(Cu(II)-IDA-CA)/q_{max}(Cu(II)-IDA-PC)) are given in Table 1. The q_{max} values for proteins on Cu(II)-IDA-CA were much larger than on Cu(II)-IDA-BC and Cu(II)-IDA-PC. The q_{max} value for angiotensin I on Cu(II)-IDA-CA was relatively large compared with those for Cu(II)-IDA-BC and Cu(II)-IDA-PC. In contrast, the q_{max} values for Car and His on Cu(II)-IDA-CA, Cu(II)-IDA-BC, and Cu(II)-IDA-PC were similar. Thus, Cu(II)-IDA-CA exhibited a higher adsorption capacity for biomacromolecules in particular (Niide et al., 2010; Oshima et al., 2011; Ougiya et al., 1998; Todd, Johnson, & Arnold, 1994). As small amino acids can access internal adsorption sites, their adsorption on Cu(II) immobilized adsorbents is proportional to the amount of Cu(II) immobilized on the adsorbents. In contrast, large proteins cannot access internal adsorption sites, and their adsorption would occur only at the surface of the adsorbents. For the adsorption of proteins containing multiple His residues, such as hemoglobin and myoglobin, the availability of Cu(II) binding sites would influence the adsorption capacity (Johnson & Arnold, 1995; Todd et al., 1994). Cu(II)-IDA-CA had a higher adsorption capacity than the other adsorbents because of the large number of Cu(II) sites available to the proteins through its higher specific surface area.

4. Conclusions

Cellulose aerogels regenerated from ionic liquid solutions exhibit large specific surface areas, even after chemical modification introducing iminodiacetic acid groups, followed by immobilization of Cu(II). Adsorption of proteins, peptides, and amino acids by immobilized metal affinity adsorption using different Cu(II) immobilized iminodiacetic acid cellulose adsorbents was studied to determine the effect of surface morphology on adsorption. The Cu(II) immobilized cellulose aerogel had a high adsorption capacity for proteins because of its high specific surface area. Thus, cellulose aerogels are attractive as polymer supports for the purification and recovery of biomacromolecules.

Acknowledgments

We are grateful for a Grant-in-Aid for Young Scientists B (No. 21760613) from the Ministry of Education, Culture, Sports, Science and Technology of Japan. This work was partly financed by the Cooperation for Innovative Technology and Advanced Research in Evolutional Areas from the Ministry of Education, Culture, Sports, Science and Technology of Japan.

References

Aaltonen, O., & Jauhiainen, O. (2009). The preparation of lignocellulosic aerogels from ionic liquid solutions. *Carbohydrate Polymers, 75*, 125–129.
Anirudhan, T. S., Rejeena, S. R., & Binusree, J. (2013). Adsorptive separation of myoglobin from aqueous solutions using iron oxide magnetic nanoparticles modified with functionalized nanocrystalline cellulose. *Journal of Chemical & Engineering Data, 58*, 1329–1339.
Cai, J., & Zhang, L. (2005). Rapid dissolution of cellulose in LiOH/urea and NaOH/urea aqueous solutions. *Macromolecular Bioscience, 5*, 539–548.
Cao, Y., Li, H., Zhang, Y., Zhang, J., & He, J. (2010). Structure and properties of novel regenerated cellulose films prepared from cornhusk cellulose in room temperature ionic liquid. *Journal of Applied Polymer Science, 116*, 547–554.
Chaga, G. S. (2001). Twenty-five years of immobilized metal ion affinity chromatography: Past, present and future. *Journal of Biochemical and Biophysical Methods, 49*, 313–334.

Chen, S., Zhou, B., Hu, W., Zhang, W., Yin, N., & Wang, H. (2013). Polyol mediated synthesis of ZnO nanoparticles templated by bacterial cellulose. *Carbohydrate Polymers*, *92*, 1953–1959.
Deng, M., Zhou, Q., Du, A., van Kasteren, J., & Wang, Y. (2009). Preparation of nanoporous cellulose foams from cellulose-ionic liquid solutions. *Materials Letters*, *63*, 1851–1854.
Dong, H., Snyder, J. F., Tran, D. T., & Leadore, J. L. (2013). Hydrogel, aerogel and film of cellulose nanofibrils functionalized with silver nanoparticles. *Carbohydrate Polymers*, *95*, 760–767.
Dupont, J., Consorti, C. S., Suarez, P. A. Z., De Souza, R. F., Fulmer, S. L., Richardson, D. P., Smith, T. E., & Wolff, S. (2002). Preparation of 1-butyl-3-methyl imidazolium-based room temperature ionic liquids. *Organic Syntheses*, *79*, 236–243.
El Seoud, O. A., Koschella, A., Fidale, L. C., Dorn, S., & Heinze, T. (2007). Applications of ionic liquids in carbohydrate chemistry: A window of opportunities. *Biomacromolecules*, *8*, 2629–2647.
Feng, L., & Chen, Z.-I. (2008). Research progress on dissolution and functional modification of cellulose in ionic liquids. *Journal of Molecular Liquids*, *142*, 1–5.
FitzPatrick, M., Champagne, P., Cunningham, M. F., & Whitney, R. A. (2010). A biorefinery processing perspective: Treatment of lignocellulosic materials for the production of value-added products. *Bioresource Technology*, *101*, 8915–8922.
Fukaya, Y., Hayashi, K., Wada, M., & Ohno, H. (2008). Cellulose dissolution with polar ionic liquids under mild conditions: Required factors for anions. *Green Chemistry*, *10*, 44–46.
Härdelin, L., Thunberg, J., Perzon, E., Westman, G., Walkenström, P., & Gatenholm, P. (2012). Electrospinning of cellulose nanofibers from ionic liquids: The effect of different cosolvents. *Journal of Applied Polymer Science*, *125*, 1901–1909.
Iguchi, M., Yamanaka, S., & Budhiono, A. (2000). Bacterial cellulose—A masterpiece of nature's arts. *Journal of Materials Science*, *35*, 261–270.
Innerlohinger, J., Weber, H. K., & Kraft, G. (2006). Aerocellulose: Aerogels and aerogel-like materials made from cellulose. *Macromolecular Symposia*, *244*, 126–135.
Isogai, A., & Atalla, R. H. (1998). Dissolution of cellulose in aqueous NaOH solutions. *Cellulose*, *5*, 309–319.
Jin, H., Nishiyama, Y., Wada, M., & Kuga, S. (2004). Nanofibrillar cellulose aerogels. *Colloids and Surfaces A: Physicochemical and Engineering Aspects*, *240*, 63–67.
Johnson, R. D., & Arnold, F. H. (1995). Multipoint binding and heterogeneity in immobilized metal affinity chromatography. *Biotechnology and Bioengineering*, *48*, 437–443.
Kadokawa, J., Murakami, M., & Kaneko, Y. (2008). A facile preparation of gel materials from a solution of cellulose in ionic liquid. *Carbohydrate Research*, *343*, 769–772.
Kalashnikova, I., Bizot, H., Cathala, B., & Capron, I. (2011). New pickering emulsions stabilized by bacterial cellulose nanocrystals. *Langmuir*, *27*, 7471–7479.
Kanemaru, K., Oshima, T., & Baba, Y. (2010). Selective recovery of histidine-containing dipeptides based on metal affinity interactions using chemically modified dextran in combination with ultrafiltration. *Reactive and Functional Polymers*, *70*, 103–109.
Lin, C.-X., Zhan, H.-Y., Liu, M.-H., Fu, S.-Y., & Lucia, L. A. (2009). Novel preparation and characterization of cellulose microparticles functionalized in ionic liquids. *Langmuir*, *25*, 10116–10120.
Liu, C.-Z., Wang, F., Stiles, A. R., & Guo, C. (2012). Ionic liquids for biofuel production: Opportunities and challenges. *Applied Energy*, *92*, 406–414.
Liu, Z., Wang, H., Li, Z., Lu, X., Zhang, X., Zhang, S., & Zhou, K. (2011). Characterization of the regenerated cellulose films in ionic liquids and rheological properties of the solutions. *Materials Chemistry and Physics*, *128*, 220–227.
Ma, H., Zhou, B., Li, H.-S., Li, Y.-Q., & Ou, S.-Y. (2011). Green composite films composed of nanocrystalline cellulose and a cellulose matrix regenerated from functionalized ionic liquid solution. *Carbohydrate Polymers*, *84*, 383–389.
Mäki-Arvela, P., Anugwom, I., Virtanen, P., Sjöholm, R., & Mikkola, J. P. (2010). Dissolution of lignocellulosic materials and its constituents using ionic liquids-a review. *Industrial Crops and Products*, *32*, 175–201.
Meli, L., Miao, J., Dordick, J. S., & Linhardt, R. J. (2010). Electrospinning from room temperature ionic liquids for biopolymer fiber formation. *Green Chemistry*, *12*, 1883–1892.
Niide, T., Shiraki, H., Oshima, T., Baba, Y., Kamiya, N., & Goto, M. (2010). Quaternary ammonium bacterial cellulose for adsorption of proteins. *Solvent Extraction Research and Development Japan*, *17*, 73–81.
Ohno, H., & Fukaya, Y. (2009). Task specific ionic liquids for cellulose technology. *Chemistry Letters*, *38*, 2–7.
Oshima, T., Kondo, K., Ohto, K., Inoue, K., & Baba, Y. (2008). Preparation of phosphorylated bacterial cellulose as an adsorbent for metal ions. *Reactive and Functional Polymers*, *68*, 376–383.
Oshima, T., Taguchi, S., Ohe, K., & Baba, Y. (2011). Phosphorylated bacterial cellulose for adsorption of proteins. *Carbohydrate Polymers*, *83*, 953–958.
Ougiya, H., Hioki, N., Watanabe, K., Morinaga, Y., Yoshinaga, F., & Samejima, M. (1998). Relationship between the physical properties and surface area of cellulose derived from adsorbates of various molecular sizes. *Bioscience Biotechnology and Biochemistry*, *62*, 1880–1884.
Pinkert, A., Marsh, K. N., Pang, S., & Staiger, M. P. (2009). Ionic liquids and their interaction with cellulose. *Chemical Reviews*, *109*, 6712–6728.
Porath, J., Carlsson, J., Olsson, I., & Belfrage, G. (1975). Metal chelate affinity chromatography, a new approach to protein fractionation. *Nature*, *258*, 598–599.
Porath, J. (1992). Immobilized metal ion affinity chromatography. *Protein Expression and Purification*, *3*, 263–281.
Quan, S.-L., Kang, S.-G., & Chin, I.-J. (2010). Characterization of cellulose fibers electrospun using ionic liquid. *Cellulose*, *17*, 223–230.
Sakamoto, T., Oshima, T., Taguchi, S., Ohe, K., & Baba, Y. (2010). Preparation of iminodiacetic acid bacterial cellulose for immobilized metal affinity chromatography. *Journal of Ion Exchange*, *21*, 141–146.
Swatloski, R. P., Spear, S. K., Holbrey, J. D., & Rogers, R. D. (2002). Dissolution of cellulose with ionic liquids. *Journal of the American Chemical Society*, *124*, 4974–4975.
Todd, R. J., Johnson, R. D., & Arnold, F. H. (1994). Multiple-site binding interactions in metal-affinity chromatography: I. Equilibrium binding of engineered histidine-containing cytochromes *c*. *Journal of Chromatography A*, *662*, 13–26.
Turner, M. B., Spear, S. K., Holbrey, J. D., & Rogers, R. D. (2004). Production of bioactive cellulose films reconstituted from ionic liquids. *Biomacromolecules*, *5*, 1379–1384.
Turner, M. B., Spear, S. K., Holbrey, J. D., Daly, D. T., & Rogers, R. D. (2005). Ionic liquid-reconstituted cellulose composites as solid support matrices for biocatalyst immobilization. *Biomacromolecules*, *6*, 2497–2502.
Ueda, E. K. M., Gout, P. W., & Morganti, L. (2003). Current and prospective applications of metal ion-protein binding. *Journal of Chromatography A*, *988*, 1–23.
Viswanathan, G., Murugesan, S., Pushparaj, V., Nalamasu, O., Ajayan, P. M., & Linhardt, R. J. (2006). Preparation of biopolymer fibers by electrospinning from room temperature ionic liquids. *Biomacromolecules*, *7*, 415–418.
Wang, H., Gurau, G., & Rogers, R. D. (2012). Ionic liquid processing of cellulose. *Chemical Society Reviews*, *41*, 1519–1537.
Wang, Z., Liu, S., Matsumoto, Y., & Kuga, S. (2012). Cellulose gel and aerogel from LiCl/DMSO solution. *Cellulose*, *19*, 393–399.
Xu, S., Zhang, J., He, A., Li, J., Zhang, H., & Han, C. C. (2008). Electrospinning of native cellulose from nonvolatile solvent system. *Polymer*, *49*, 2911–2917.
Yanagisawa, M., Shibata, I., & Isogai, A. (2004). SEC-MALLS analysis of cellulose using LiCl/1,3-dimethyl-2-imidazolidinone as an eluent. *Cellulose*, *11*, 169–176.
Zhang, H., Wang, Z., Zhang, Z., Wu, J., Zhang, J., & He, J. (2007). Regenerated-cellulose/multiwalled-carbon-nanotube composite fibers with enhanced mechanical properties prepared with the ionic liquid 1-allyl-3-methylimidazolium chloride. *Advanced Materials*, *19*, 698–704.